UDC669.14.018.26:629.11.011.5

Development of New Formable Cold-Rolled Sheet Steels for Automobile Body Panels

Atsushi Itami*1 Hirohide Asano*1
Kohsaku Ushioda*1 Yoshitaka Kimura*2
Noritoshi Kimura*2 Kazuo Koyama*1

Abstract:

New super-formable cold-rolled sheet steel and bake-hardenable sheet steel with good formability were developed. Their $\bar{r}$ value and n value, important material properties for automobile body panel applications, are higher than those of conventional interstitial-free (IF) steels. The super-formable cold-rolled sheet steel with $\bar{r} = 2.5$ and $n = 0.27$ can be commercially produced by hot-rolled band grain refinement and precipitation control. The role of hot-band grain refinement in enhancing the $\bar{r}$ value is discussed. The bake-hardenable sheet steel with good formability can be stably manufactured by leaving excess carbon in solid solution. The possibility of eliminating compositional constraint on the galvannealing of high-strength cold-rolled sheet steels by a new process is discussed.

1. Introduction

Sheet steels for automobile body exposed panels, such as door panels and fenders, and unexposed panels, such as floor and dashboard panels require deep drawability, stretchability, stiffness, dent resistance, and corrosion resistance. These property requirements can be met by interstitial-free (IF) steel[1]. The IF steel was invented in the late 1960s in Japan. The IF steel, which has a high $\bar{r}$ value and n value, is free from dependence on the heating rate during annealing, and does not require any special heat treatment for carbon precipitation. These characteristics allow the IF steel to be easily manufactured on a continuous hot-dip galvanizing line without an overaging zone. With some latest improvements[2,3] they have rapidly expanded the scope of application of the IF steel into cold-rolled, hot-dip galvanized and electrogalvanized sheet products for automotive use. The IF steel is now a predominant type of steel for automobile body panels.

The sheet steels described here are improved versions of the IF steel with much more sophisticated properties. Their development was prompted by the needs for super-formable cold-rolled sheet steel and high-strength and formable cold-rolled sheet steel capable of answering the design and weight reduction requirements of the automobile industry. Concerning the super-formable cold-rolled sheet steel, descriptions are made of the increase of formability to the highest possible extent on an industrial basis by improving steel purity and controlling the texture development. Concerning the high-strength cold-rolled sheet steel, descriptions deal with the results of the commercial production of cold-rolled sheet steel with good formability and bake hardenability employing the method of leaving carbon in an

*1 Technical Development Bureau
*2 Kimitsu Works

excess amount relative to titanium and niobium. Lastly, the future possibility of shifting to high-strength steel as the galvannealed steel stock by eliminating the existing steel compositional constraint is discussed.

2. Super-Formable Cold-Rolled Sheet Steel

2.1 Basic concept

The $\bar{r}$ value of a sheet product is governed by its texture and improves with increasing intensity of ND//<111> (ND//<hkl> is hereinafter referred to as {hkl}). ND denotes the direction normal to the rolling plane of the sheet. Many published reports are available about the recrystallization texture control of cold-rolled steel[4-8]. According to these studies, the {111} recrystallized grains and {110} recrystallized grains preferentially nucleate at and within the grain boundaries of the cold-rolled sheet, respectively, in the initial recrystallization stage[6,7]. To enhance the $\bar{r}$ value, the grain size of the hot-rolled band must be refined. Particularly with high-purity steel, it should be noted that grains in the hot-rolled band are susceptible to coarsening. In the grain growth stage, the {111} texture develops[8], so that it is necessary to reduce the contents of solute elements objectionable to grain growth and to coarsen precipitates. The precipitates and hot-rolled band grain size are govered by the hot rolling conditions, and hot rolling occupies an important position in achieving a still higher $\bar{r}$ by improving steel purity. The n value is governed by steel purity and grain size after annealing[9]. To obtain a high n value, the steel purity must be enhanced and sufficient grain growth be ensured. Hot rolling conditions are important in this connection. Titanium-bearing high-purity steel was melted in the production furnace in order to achieve a high $\bar{r}$ value[10], and mill and laboratory tests were conducted to clarify the effects of hot rolling conditions on the $\bar{r}$ value and n value of hot the steel.

2.2 Test methods and results

Steel A of the chemical composition given in **Table 1** was hot rolled, cold rolled, and continuously annealed under the conditions given in **Table 2**. In the hot rolling stage, the steel was rapidly cooled immediately after finish rolling[10]. **Fig. 1** shows the effect of the finishing temperature (FT) on the $\bar{r}$ value. The $\bar{r}$ value improves with decreasing finishing temperature, and the improvement of the r_{45} value is particularly noticeable. When the steel was conventionally cooled, $\bar{r}$ = 2.5 was obtained at the finishing temperature of about 910°C. The immediately and rapidly cooled steel had a smaller hot-rolled band grain size than the conventionally cooled steel, and the smaller grain size improved the $\bar{r}$ value of the final products. The $\bar{r}$ value and recrystallization texture are arranged by the hot-rolled band grain size in **Fig. 2**.

Table 1 Chemical compositions of test steels (mass%, *: mass ppm)

Steel	C*	Si	Mn	P	S	Al	Ti	B*	N*
A	14	0.008	0.13	0.008	0.003	0.017	0.050	3	15
B	16	0.009	0.06	0.003	0.004	0.037	0.045	2	15
C	25	0.013	0.14	0.011	0.009	0.038	0.054	3	18
D	12	0.007	0.12	0.008	0.003	0.021	0.051	3	14

Table 2 Manufacturing conditions of steel A

Hot rolling				Cold rolling	Continuous annealing	
SRT,℃	FT,℃	CT,℃	Thickness (mm)	Thickness (mm)	ST(℃)	OA(℃)
1,100–1,150	900–960	670–720	5.5	1.2	850	350
			6.5	1.6		

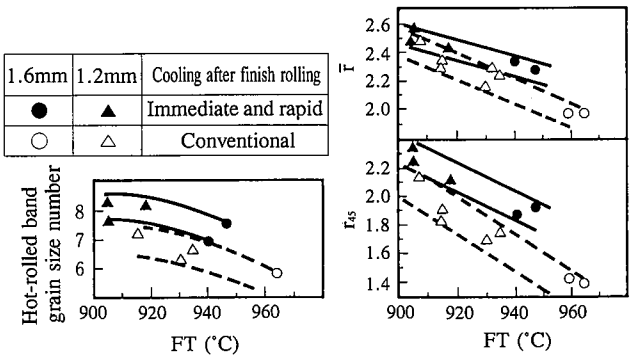

Fig. 1 Relationship of finishing temperature (FT) with $\bar{r}$ value and hot-rolled band grain size

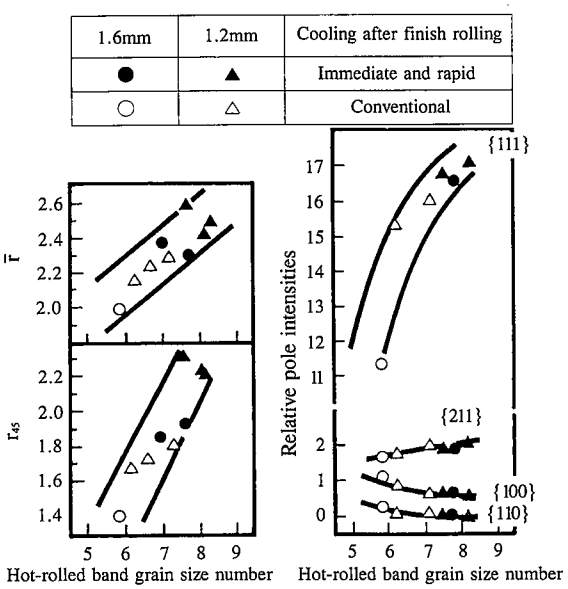

Fig. 2 Effect of hot-rolled band grain size on $\bar{r}$ value and recrystallization texture

Immediate and rapid cooling refined the hot-rolled band grain size to about No. 8 and increased the $\bar{r}$ value to 2.5. These results are endorsed by the recrystallization texture. The grain refinement of the hot-rolled band texture markedly raises the intensity of the {111} recrystallized grains and lowers that of the {100} and {110} recrystallized grains.

Next, steels B and C of the chemical compositions listed in **Table 1** were reheated at 1,056 to 1,188°C, finish rolled to 4.5 mm at 905°C, and coiled at 750°C at the mill. These steels were not immediately cooled after finish rolling. Each hot-rolled band was cold rolled to 0.8 mm and annealed at 875°C in the laboratory. Steel B is as high in purity as steel A, and steel C is higher in carbon and nitrogen and lower in purity than steel B. The absence of "orange peel" surface defect by annealing at 875°C was confirmed. **Fig. 3** shows the relationship between the slab reheating temperature (SRT) and the $\bar{r}$ value[11]. The $\bar{r}$ value increased with decreasing carbon content and slab reheating temperature. Steel B, which is a ultrahigh-purity steel, exhibits an extremely high $\bar{r}$ value, and steel C markedly improves in the $\bar{r}$ value with decreasing slab reheating temperature. **Fig. 4**[11] shows the relationship of the slab reheating temperature with the n value. Steel B exhibited a high n value of 0.28, irrespective of

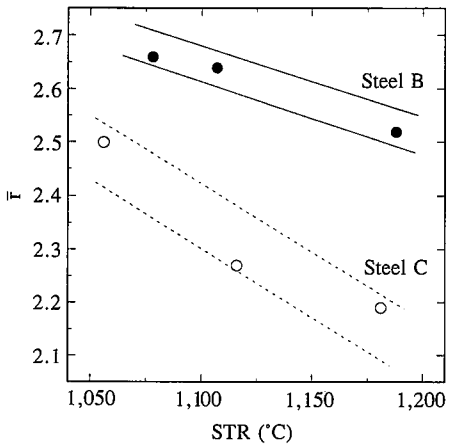

Fig. 3 Relationship between slab reheating temperature (SRT) and r̄ value

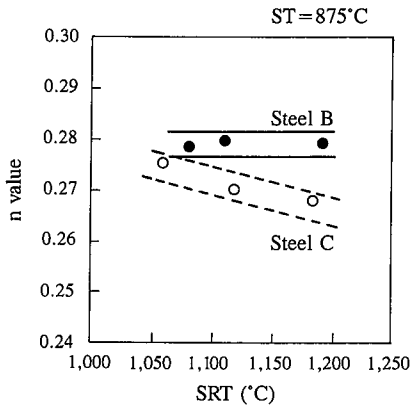

Fig. 4 Relationship between slab reheating temperature (SRT) and n value

the slab reheating temperature, while steel C increased in the n value with decreasing reheating temperature.

The above-mentioned study results led to the successful trial production of super-formable sheet steel with the r̄ value of 2.5 and n value of 0.27, as shown in **Table 3**. A separate report[12] presents in detail the results of evaluation made of the performance of the new cold-rolled sheet steel.

2.3 Discussion

The super-formable cold-rolled sheet steel was produced through the grain refinement and precipitate control of the hot-rolled band, involving the optimization of finishing temperature and immediate and rapid cooling after hot rolling[13]. The relationship between the grain refinement of the hot-rolled band and the r̄ value is discussed here.

Since the r̄ value is determined by the texture, the grain refinement of the hot-rolled band by immediate and rapid cooling is believed to change the recrystallization behavior of the cold-rolled strip. Hot-rolled bands with their grain size changed by immediate and rapid cooling at the mill were investigated for

Table 3 Properties of super-formable cold-rolled sheet steel

Thickness (mm)	YP (N/mm²)	TS (N/mm²)	El (%)	r̄	n
0.8	116	273	53.8	2.63	0.278
1.2	121	271	56.8	2.63	0.272
1.6	126	280	57.2	2.58	0.273

Table 4 Hot rolling conditions of steel D

No.	SRT(°C)	FT(°C)	Immediate and rapid cooling	CT(°C)	Grain size No.
D-A	1,151	915	With	725	6.7
D-B	1,151	904	Without	715	8.0

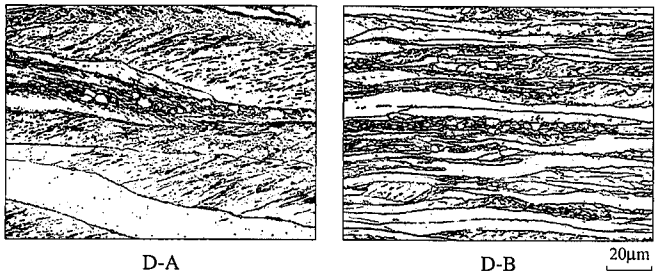

Photo 1 Appearance of recrystallized ferrite from grain boundaries and dark-etched regions (at annealing temperature of 660°C)

recrystallization behavior after cold rolling. Steel D of the chemical composition given in **Table 1** was hot rolled under the conditions of **Table 4**. Immediate and rapid cooling refined the steel by changing the grain size number from 6.7 (for steel D-A) to 8.0 (for steel D-B). The hot-rolled bands were cold rolled from 6.5 to 1.6 mm and were annealed at 500 to 800°C in the laboratory.

The recrystallization start temperature (the temperature at which recrystallized ferrite appears) was about 660°C for steel D-A and 640°C for steel D-B. The recrystallization finish temperature (the temperature at which the cold-rolled structure completely disappears) was about 780°C for steel D-A and 760°C for steel D-B. The finer the grain size of the hot-rolled band, the lower became the recrystallization temperature. Recrystallized ferrite predominantly appeared at the initial grain boundaries and in the dark-etched regions[14] in the cold rolled strip, as shown in **Photo 1**. Recrystallization in the bright-etched regions proceeded in such a way that unrecrystallized ferrite grains in the bright-etched regions were consumed by recrystallized ferrite grains nucleated at the initial grain boundaries and in the dark-etched regions. As shown in **Fig. 5**, steel D-B was consistently high in the intensity of the {111} recrystallized grains from cold rolling to grain growth. The ferrite grain size number at the annealing tempera-

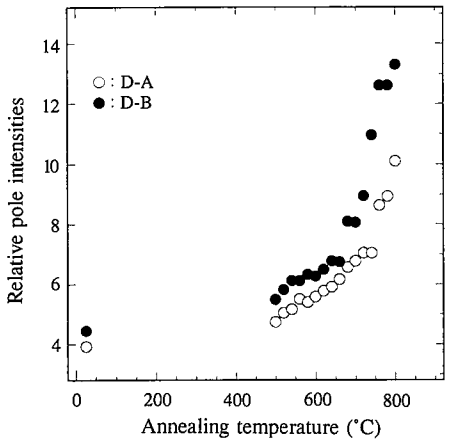

Fig. 5 Influence of hot-rolled band grain size on recrystallization of {111}-oriented grains

ture of 800°C, which falls in the grain growth stage, was 8.0 for steel D-A and 8.9 for steel D-B.

The effect of hot-rolled band grain refinement on the $\bar{r}$ value is discussed here according to the above-mentioned experimental results. In the cold rolling stage, steel D-B was higher in the intensity of {111} recrystallized grains as shown in **Fig. 5**. This agrees with the experimental finding of Abe[14]. In other words, the effect of increased cold rolling reduction in improving the $\bar{r}$ value[15] is attributable to the grain refinement of the hot-rolled band microstructure. Next, the dark-etched regions and grain boundaries (regions nearby) in the cold-rolled strip are believed to be higher in dislocation density than the other regions[16] and to reduce the recrystallization temperature by affording many recrystallization nuclei. Matsudo et al. explained the $\bar{r}$ value in the product stage as the sum of the $\bar{r}$ value in the recrystallization finish stage and the $\bar{r}$ value in the grain growth stage[17]. The grain refinement of the hot-rolled band microstructure is thought to have contributed to the improvement in the $\bar{r}$ value by grain growth through a low recrystallization temperature. These findings show that the grain refinement of the hot-rolled band microstructure improves the $\bar{r}$ value by 1) developing the cold-rolled strip texture; 2) increasing the nucleation frequency of the {111} recrystallized grains; and 3) lowering the recrystallization temperature and affording much time for ferrite grain growth.

3. Bake-Hardenable Sheet Steel with Good Formability

3.1 Basic concept of bake hardenability

Bake hardening utilize strain-age hardening by interstitial solute elements and solute carbon in particular. The control of solute carbon is important in this respect. The solute carbon may be controlled by 1) leaving carbon in an excess amount relative to titanium and niobium in the steelmaking stage[18]; 2) completely tying up carbon by titanium or niobium in the hot rolling stage and redissolving titanium or niobium carbides and leaving the solute carbon in solid solution by high-temperature annealing in the continuous annealing stage[19,20]; and 3) a compromise between methods 1) and 2)[21]. By method 1), bake hardenability is stably obtained irrespective of the annealing temperature or subsequent cooling pattern, but this stands on the condition that the desired carbon, titanium and niobium contents should be achieved with high accuracy in the steelmaking process. Method 2) can provide stable bake hardenability because the change in the solute carbon content in relation to the variability of steel chemistry is smaller than for method 1) as shown in **Fig. 6**, and can impart high formability as well, because the absence of solute carbon in the cold rolling stage. Method 2), however, involves many problems to be solved, such as the need for annealing at an extremely high temperature in the continuous annealing stage and attention to the reprecipitation of carbides on cooling after high-temperature annealing. Accordingly, descriptions here concern method 1) whereby stable bake hardenability and high formability can be obtained by controlling a niobium-to-carbon atomic ratio of about 0.9[18].

3.2 Properties of trially produced sheet steel

3.2.1 Production results of cold-rolled sheet steels and discussion

According to the bake hardenability considerations described in the preceding section, high-strength sheet steel was trially produced with the chemical compositions and process conditions given in **Tables 5** and **6**, respectively. A tensile strength of 340

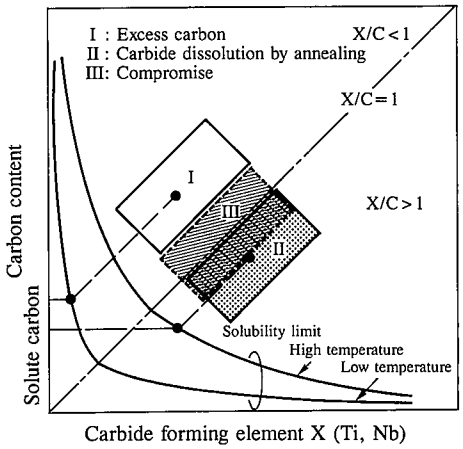

Fig. 6 Methods for imparting bake hardenability to IF steel

N/mm² was targeted, and to prevent any rise in yield strength, the phosphorus content was held low, and the manganese content was kept high[20]. In the hot rolling stage, the steel was reheated at a low temperature and coiled at a high temperature. As a result, there were obtained sheets with a bake-hardening yield strength increment of more than 40 N/mm² and an $\bar{r}$ value of 2.0 to 2.4, as shown in **Table 7**.

To investigate the bake hardenability of the newly developed steel in more detail, the above-mentioned as-cold-rolled steel was studied in the laboratory as to the effects of the soaking temperature (ST), rapid cooling start temperature (2S), and overaging temperature (OA) on bake hardenability. Sheet steel with a niobium-to-carbon atomic ratio of 2.10 was used for reference. As shown in **Fig. 7**(a), the new steel changes little in the bake-hard-

Table 5 Chemical compositions of test steels (mass%, *: mass ppm)

Steel	C*	Si	Mn	P	S	Al	Nb	Ti	N*	Nb/C
1	16	0.01	0.70	0.040	0.0058	0.027	0.011	0.006	20	0.92
2	20	0.01	0.68	0.039	0.0043	0.024	0.012	0.006	17	0.78

Nb/C is niobium-to-carbon atomic ratio.

Table 6 Hot rolling, cold rolling, and continuous annealing conditions of test steels

Steel	Portion	Hot rolling			Cold rolling	Continuous annealing		
					Thickness (mm)			
		SRT(°C)	FRT(°C)	CT(°C)	(Reduction)	ST(°C)	OA(°C)	SP(%)
1	T	1,160	902	761	4.0/0.65	863	290	0.8
	B		906	745	(83.8%)	888	311	0.8
2	T	1,155	897	751	4.0/0.65	845	284	0.8
	M		910	739	(83.8%)	875	305	0.8
	B		905	745		873	300	0.8

Portion: T for head end, M for middle, and B for tail end of hot coil.

Table 7 Tensile properties of trially produced sheet products

Steel	Portion	YP(N/mm²)	TS(N/mm²)	El(%)	$\bar{r}$	BH(N/mm²)
1	T	205	346	42	1.92	47
	B	188	342	43	2.05	42
2	T	218	359	43	2.04	53
	M	242	339	43	2.39	66
	B	198	344	44	2.06	74

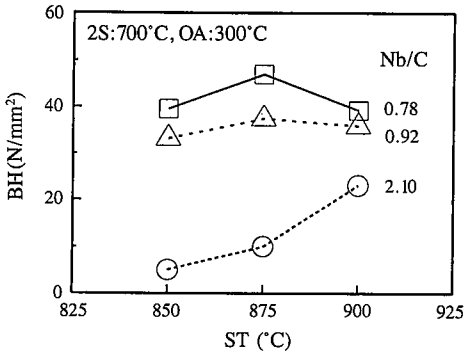

(a) Effect of soaking temperature (ST) on bake hardenability (BH)

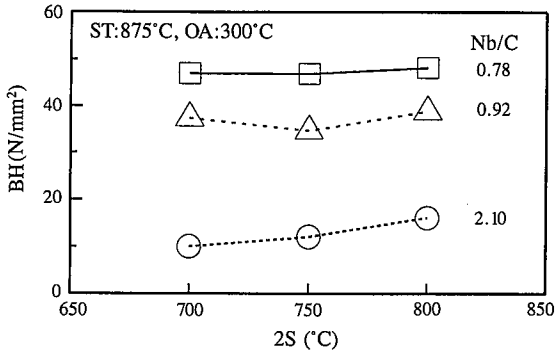

(b) Effect of rapid cooling start temperature (2S) on bake hardenability (BH)

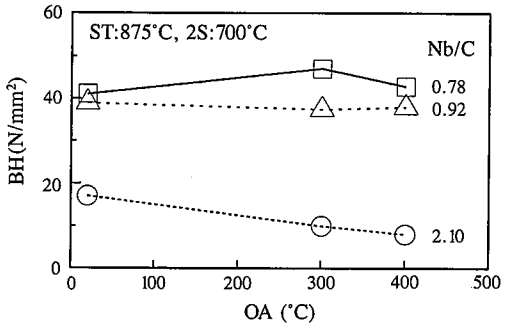

(c) Effect of overaging temperature (OA) on bake hardenability (BH)

Fig. 7 Effect of annealing conditions on bake hardenability

ening yield strength increment in the annealing temperature range of 850 to 900℃ and exhibits stable bake hardenability. The reference steel improves in the bake-hardening yield strength increment with increasing annealing temperature, probably because increasing the annealing temperature redissolves niobium carbide (NbC) and increases the amount of solute carbon. As evident from **Figs.** 7(b) and 7(c), the effects of the rapid cooling start temperature and the overaging temperature on bake hardenability are smaller for the new steel than for the reference steel. The change in the bake hardenability of the reference steel may be explained by the precipitation of niobium carbide on slow cooling prior to the start of rapid cooling, precipitation of iron carbide during overaging[21], or grain-boundary segregation of carbon.

The dent resistance of the newly developed steel is shown as arranged by (YP + WH (work hardening; 2% stretching flow

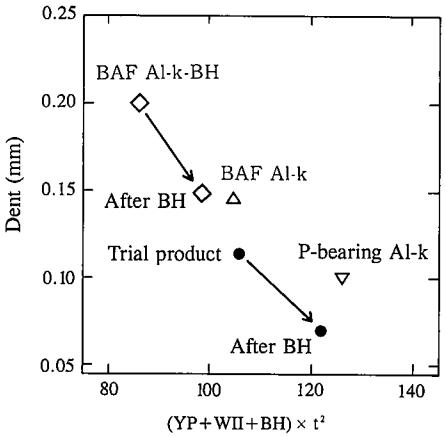

Fig. 8 Post-forming yield point with allowance for sheet thickness and dent

stress increment) + BH) × t² in **Fig. 8**. A 200 mm square specimen was strained by stretching over a 100-mm diameter flat-bottomed punch, a 50-mm diameter indenter was forced into the specimen under the load of 200 N, and the dent resistance of the specimen was evaluated by the amount of the resultant indentation. When bake hardened, the trially produced sheet steel with a tensile strength of 340 N/mm² (t = 0.65 mm) exhibited dent resistance equal to or higher than that of batch annealed phosphorus-bearing aluminum-killed steel with a tensile strength of 370 N/mm² (t = 0.7 mm). In this way, the newly developed steel offers good formability and high dent resistance after paint baking, making it possible to use thinner gauges than in the past.

3.2.2 Production results of galvannealed sheet steels

Steels 1 and 2 of the chemical compositions listed in **Table 5** were hot rolled to a thickness of 4.5 mm under conditions practically identical to those given in **Table 6**. The cold rolling and hot-dip galvanizing conditions are presented in **Table 8**. As a result, there were obtained galvannealed sheets with excellent formability and bake hardenability, as shown in **Table 9**.

4. Future Outlook

Manufacture of high-strength sheet steel requires large amounts of strengthening elements. The considerations that deserve special mention here are the phosphatability of cold-rolled steel and the zinc coating adhesion (wettability) and zinc alloying rate of galvannealed steel. It is confirmed that the phos-

Table 8 Cold rolling and continuous hot-dip galvanizing conditions

Steel	Cold rolling	Continuous hot-dip galvanizing		
	Thickness (mm) (Reduction)	RF(℃)	Bath temperature(℃)	Strip temperature(℃)
1	4.5/0.8(82%)	840	460	500
2	4.5/0.8(82%)	843	460	490

Table 9 Tensile properties of test steels (at mid-length of coil)

Steel	YP (N/mm²)	TS (N/mm²)	El (%)	n value	r̄ value	BH (N/mm²)	WH (N/mm²)
1	224	350	42	0.23	1.66	35	38
2	224	354	42	0.23	1.73	30	40

phatability of high-strength cold-rolled steel with a high silicon content can be improved by adding calcium in the steelmaking process and by coating the strip surface with sulfur before annealing[22]. Alloying elements have a large influence on the zinc coating adhesion and zinc alloying[23] and constitute serious compositional constraints for the commercial production of high-strength galvannealed steel. When silicon and manganese additions are made, for example, the annealing furnace atmosphere in the continuous hot-dip galvanizing line is reducing for iron but oxidizing for silicon and manganese, as shown in **Fig. 9**[24]. The resultant concentration of silicon and manganese oxides on the strip surface reduces the zinc adhesion to the steel substrate[25]. **Fig. 9** shows that the oxidation of steel elements can be suppressed, depending on the heating temperature and the ambient conditions. If the constraint of major solid-solution strengtheners, such as silicon and manganese, is eliminated, the chemical composition of high-strength galvannealed steel can be freely designed before manufacture. This issue is discussed below as one of the future outlooks.

In the conventional nonoxidizing furnace-reducing furnace (NOF-RF) process, high-silicon-manganese steel strip is covered with an iron oxide film in the heating zone. In the reducing zone, the silicon and manganese are concentrated as the complex oxide $MnSiO_2$ on the strip surface, and $MnSiO_2$ deteriorates the wettability of the strip surface with zinc[25]. However, a pure iron layer can be formed on the strip surface in the reducing zone by raising the air ratio in the heating zone from the normal level of 0.9 to 1.05 and increasing the iron oxide film thickness in the heating zone as shown in **Fig. 10**. The optimum condition is immersion in the zinc coating pot of the strip at the completion of reduction as shown in **Fig. 10**. When the oxide film remains, peeling is likely to occur at or near the interface between the oxide film and the pure iron layer. When silicon is concentrated in the strip surface, the zinc coating cannot tightly adhere to the steel substrate. This is observed during operation with a conventional air ratio. In the laboratory, 1.0%Si-1.2%Mn steel was heated over an air ratio range of 0.90 to 1.05 and a temperature range of 500 to 700℃ (as-heated specimens), and was reduced and held in a nitrogen atmosphere for 120 s (heated and reduced specimens). The complex oxide $MnSiO_2$ concentrated in the steel surface was evaluated as the amount of silicon by glow discharge

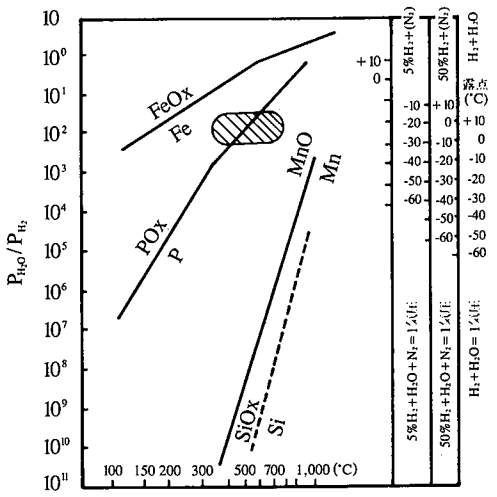

Fig. 9 Oxidation-reduction equilibrium in H_2-H_2O-N_2 atmosphere

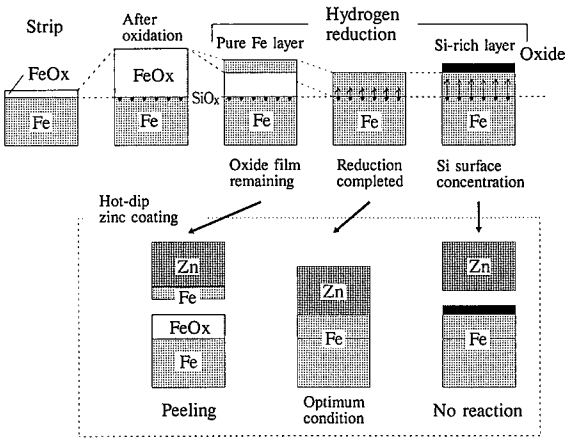

Fig. 10 Air ratio control and oxide film

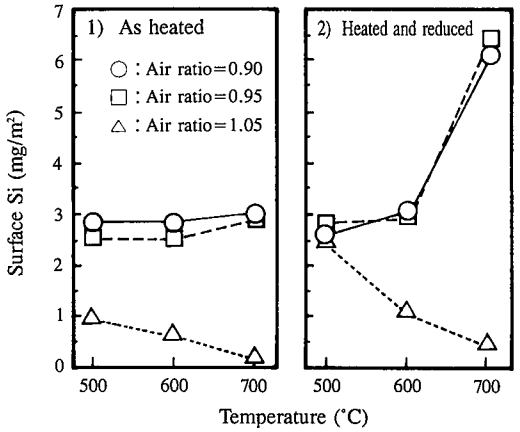

Fig. 11 Effect of air ratio on silicon concentration

spectroscopy (GDS). The results are given in **Fig. 11**[26]. The silicon and manganese are concentrated by reduction. If the air ratio is increased during heating, the concentration of silicon and manganese by reduction cannot occur. It is thus important to control the thickness of the iron oxide film in the heating zone. It is confirmed at the mill that the iron oxide film thickness can be measured by an in-line oxide film thickness meter[27] and that the zinc coating adhesion of high-silicon-manganese steel can be assured by this technique[26].

5. Conclusions

Super-formable cold-rolled sheet steel, formable bake-hardenable sheet steel, and the possibility of eliminating compositional constraint on the galvannealing of high-strength sheet steel by a new process have been discussed. The results may be summarized as follows:

For the super-formable cold-rolled sheet steel,

(1) Sheet products with $\bar{r} = 2.5$ and $n = 0.27$ can be commercially manufactured from high-purity steel by refining the grain size of the hot-rolled band and controlling precipitates.

(2) The grain refinement of the hot-rolled band is believed to enhance the $\bar{r}$ value by 1) promoting the evolution of the cold-rolled texture; 2) improving the nucleation frequency of the {111} recrystallized grains; and 3) affording large grain growth allowance after recrystallization.

For the formable bake-hardenable sheet steel,

(3) High-strength cold-rolled sheet steel and cold-rolled galvannealed sheet steel with good formability and high bake hardenability can be commercially produced by leaving excess carbon in solid solution in the steelmaking process.
For the elimination of compositional constraint on the galvannealing of high-strength sheet steel,

(4) The complex oxide $SiMnO_3$ that hampers the zinc coating adhesion of high-strength sheet steel is formed in the reducing zone. Its concentration can be prevented by increasing the air ratio to increase the iron oxide film thickness in the heating zone.

(5) The thickness of the iron oxide film can be controlled by an in-line oxide film thickness meter to ensure the desired zinc coating adhesion of high-silicon-manganese steel.

References

1) Fukuda, N., Shimuzu, M.: J. Jpn. Soc. Technol. Plast. 13, 841 (1972)
2) Hashimoto, O., Satoh, S., Tanaka, T.: Tetsu-to-Hagané. 67 (11), 1962 (1981)
3) Yamada, M., Tokunaga, Y., Yamamoto, M.: Tetsu-to-Hagané. 73 (8), 1049 (1987)
4) Nagashima, S.: Shugousoshiki ("Textures" in Japanese). First Edition. Tokyo, Maruzen, 1984
5) Research Committee on Ultralow-Carbon Sheet Steels, Society on Basic Research: Gokuteitanso Kohan no Kinzokugaku ("Metallurgy of Ultarlow-Carbon Sheet Steels" in Japanese). Tokyo, Iron and Steel Institute of Japan, 1993
6) Abe, M. et al.: Trans. Jpn. Inst. Met. 23, 718 (1982)
7) Ushioda, K., Abe, M.: Tetsu-to-Hagané. 70 (1), 96 (1984)
8) Hutchinson, W.B.: International Metals Review. 29, 25 (1984)
9) Masui, H., Kawaharada, M., Takechi, H.: Tetsu-to-Hagané. 58 (8), 1096 (1972)
10) Matsuzu, N. et al.: CAMP-ISIJ. 3 (6), 1816 (1990)
11) Suzuki, T. et al.: CAMP-ISIJ. 7 (6), 1690 (1994)
12) Itami, A. et al.: SAE Tec. Pap. 930783. 1993
13) Ushioda, K. et al.: Forum Book of International Forum for Physical Metallurgy of IF Steels. Tokyo, May 1994, ISIJ
14) Abe, M.: Dr. Eng. Thesis of Kyoto University. 1976
15) Itoh, K. et al.: Tetsu-to-Hagané. 70 (15), 1878 (1984)
16) Abe, M., Kokabu, Y., Hayashi, Y., Hayami, S.: Trans. JIM. 23, 718 (1982)
17) Matsudo, K., Shimomura, T.: Tetsu-to-Hagané. 56 (1), 28 (1970)
18) Yamada, M., Tokunaga, Y., Ito, K.: Seitetsu Kenkyu. (322), 90 (1986)
19) Kawasaki, K. et al.: Tetsu-to-Hagané. 79 (1), 76 (1993)
20) Ushioda, K., Yoshinaga, N., Akisue, O.: CAMP-ISIJ. 5 (6), 2050 (1992)
21) Satoh, S. et al.: Kawasaki Seitetsu Giho. 23, 293 (1991)
22) Itami, A. et al.: CAMP-ISIJ. 2 (6), 1927 (1989)
23) Nishimoto, A., Inagaki, J., Nakaoka, K.: Tetsu-to-Hagané. 68 (9), 1404 (1982)
24) Meada, Y.: Hyomen Shori Gijutsu Soran ("Handbook of Surface Treatment Technology" in Japanese). First Edition, Tokyo, Sangyo Gijutsu Service Center, 1987, p. 16
25) Hirose, Y. et al.: 88th and 89th Nishiyama Memorial Lecture. Tokyo, Iron and Steel Institute of Japan, 1983, p. 229
26) Kimura, Y. et al.: Collected Abstracts of 1993 Autumn Meeting of Japan Institute of Metals, 1993, p. 96
27) Tanaka, T.: Keiso ("Instrumentation" in Japanese). 32 (9), 69 (1989)